Excitonic effects in the miniband formation of graded-gap superlattices

N. Linder
Institut für Technische Physik I, Universität Erlangen-Nürnberg, Erwin-Rommel-Strasse 1, D-91058 Erlangen, Germany

U. Behn
Fachhochschule Schmalkalden, Blechhammer 4 und 9, D-98564 Schmalkalden, Germany

F. Agulló-Rueda
Instituto de Ciencia de Materiales de Madrid, CSIC, Cantoblanco, E-28049 Madrid, Spain

H. T. Grahn, L. Schrottke, and K. H. Ploog
Paul-Drude-Institut für Festkörperelektronik, Hausvogteiplatz 5-7, D-10117 Berlin, Germany
(Received 15 October 1996)

The formation of an electron miniband has been investigated in two differently realized graded-gap superlattices (SL's). The first SL is compositionally graded, while the second system consists of layers with different well and barrier thicknesses. The formation of the miniband in the conduction band is studied experimentally by photocurrent (PC), electroreflectance (ER), and photoluminescence (PL) spectroscopy. The experimental results are compared with the field dependence of calculated differential absorption spectra for both systems. In the compositionally graded SL, the formation of a miniband in the conduction band at finite electric fields can be clearly observed in the ER spectra. However, in the well width graded system, both the PC and the ER spectra are dominated by excitonic effects, which prevent the direct observation of the miniband formation. [S0163-1829(97)04223-9]

I. INTRODUCTION

Multiple quantum well (QW) and superlattice (SL) structures fabricated from different semiconductors have been extensively investigated over the last decade. The formation of and the transport in minibands,[1] the localization of the conduction band states by an applied electric field, i.e., the Wannier-Stark localization,[2] as well as resonant tunneling have been studied.[3,4] A review of the electronic properties of semiconductor superlattices can be found in Ref. 5.

Graded-gap SL's were proposed more than 10 years ago to improve the electric behavior of specific devices, e.g., avalanche photodiodes.[6] Over the years graded-gap SL's have been used for many different applications such as Schottky diodes,[7] distributed Bragg reflectors in vertical cavity surface emitting lasers,[8] nonalloyed Ohmic contacts,[9] and very recently in the quantum cascade laser (QCL).[10] A new photorefractive effect resulting from the spatial separation of electrons and holes in a specifically designed graded-gap SL was also reported.[11] However, the only structure relying on the formation of a miniband in the conduction band at finite electric fields is the QCL.

Although the formation of the miniband in a graded-gap SL can be easily calculated, the experimental verification is rather difficult, since the structure is not truly periodic. The grading can be achieved either by changing the content of one constituent material in a ternary semiconductor compound using a fixed layer thickness for well and barrier (compositional grading) or by changing the well and barrier thicknesses (thickness grading) in order to keep the coupling between two adjacent wells constant. Recently, both approaches were reported, the compositionally graded[12] and the thickness graded SL.[13] In order to unambiguously prove the formation of a miniband at finite electric fields, optical experiments are necessary, since the transport characteristics usually show only a strong increase in the current at the corresponding field strength.

In this paper we will compare the formation of a miniband in the conduction band in a compositionally graded SL and in a thickness graded SL. Photocurrent (PC), electroreflectance (ER), and photoluminescence (PL) spectroscopy are used for the experimental observation of miniband formation. Calculations of the field dependence of the differential absorption coefficient are performed in order to identify the region of miniband formation and to determine the field range of the transition region, i.e., the region of Wannier-Stark localization. Due to the special design of graded-gap SL's, the miniband forms at finite electric fields. For one polarity it forms in the conduction band, for the other polarity in the valence band. Therefore, in contrast to conventional SL's, the miniband in the conduction band and the miniband in the valence band are not present in the same field range. Furthermore, the transition regime between localized and extended states, i.e., the Wannier-Stark regime, can be confined to a much narrower field range than in conventional SL's. In the compositionally graded system the miniband formation can be unambiguously observed in the ER spectra due to the absence of excitonic effects. However, if the graded gap is realized by changing the well and barrier thickness, both, PC and ER spectra are dominated by excitonic effects. Under this condition the formation of the miniband is difficult to observe in the optical spectra. However, calculations of the energy band structure and the resulting differential absorption coefficient neglecting excitonic ef-

TABLE I. Layer sequence of the compositionally graded superlattice. d denotes the nominal layer thickness.

Well	d (nm)	Material
	2.0	$Al_{0.30}Ga_{0.70}As$
1	4.0	GaAs
	2.0	$Al_{0.33}Ga_{0.67}As$
2	4.0	$Al_{0.03}Ga_{0.97}As$
	2.0	$Al_{0.36}Ga_{0.64}As$
3	4.0	$Al_{0.06}Ga_{0.94}As$
	2.0	$Al_{0.39}Ga_{0.61}As$
4	4.0	$Al_{0.09}Ga_{0.91}As$
	2.0	$Al_{0.42}Ga_{0.58}As$
5	4.0	$Al_{0.12}Ga_{0.88}As$
	2.0	$Al_{0.45}Ga_{0.55}As$
6	4.0	$Al_{0.15}Ga_{0.85}As$
	2.0	$Al_{0.48}Ga_{0.52}As$
7	4.0	$Al_{0.18}Ga_{0.82}As$
	2.0	$Al_{0.51}Ga_{0.49}As$
8	4.0	$Al_{0.21}Ga_{0.79}As$
	2.0	$Al_{0.54}Ga_{0.46}As$
9	4.0	$Al_{0.24}Ga_{0.76}As$
	2.0	$Al_{0.57}Ga_{0.43}As$
10	4.0	$Al_{0.27}Ga_{0.73}As$
	2.0	$Al_{0.60}Ga_{0.40}As$
11	4.0	$Al_{0.30}Ga_{0.70}As$
	2.0	$Al_{0.63}Ga_{0.37}As$
12	4.0	$Al_{0.33}Ga_{0.67}As$
	2.0	$Al_{0.66}Ga_{0.34}As$
13	4.0	$Al_{0.36}Ga_{0.64}As$
	2.0	$Al_{0.69}Ga_{0.31}As$
14	4.0	$Al_{0.39}Ga_{0.61}As$
	2.0	$Al_{0.72}Ga_{0.28}As$
15	4.0	$Al_{0.42}Ga_{0.58}As$
	2.0	$Al_{0.75}Ga_{0.25}As$

fects clearly demonstrate the formation of a miniband in the conduction band for both types of graded-gap SL's.

II. EXPERIMENT

The investigated superlattices are embedded in the intrinsic region of a p^+-i-n^+ diode. The samples are fabricated by molecular beam epitaxy on n^+ (001) GaAs substrates. In the compositionally graded superlattice each of the 15 periods consists of a pair of $Al_xGa_{1-x}As/Al_{0.3+x}Ga_{0.7-x}As$ layers with constant well and barrier thickness of 4.0 and 2.0 nm, respectively. Between each period the Al mole fraction x is increased by 0.03. The full structure is shown in Table I. The other graded-gap superlattice consists of 8 periods of GaAs wells and $Al_{0.35}Ga_{0.65}As$ barriers with varying well and barrier thickness as shown in Table II, which we will refer to as the thickness graded SL. Between the doped layers and the superlattice, there is in both cases an enlarged GaAs well of 25-nm thickness. The p^+ (n^+) layer consists of a carbon- (silicon-) doped $Al_{0.6}Ga_{0.4}As$ (compositionally graded) or $Al_{0.5}Ga_{0.5}As$ (thickness graded) layer with a doping density of 3×10^{19} cm^{-3} (2×10^{18} cm^{-3}). There is an $Al_xGa_{1-x}As$ graded layer of 70-nm width between the contact layer and the enlarged well. The samples are structured into mesas of 120-μm diameter. AuGe/Ni and Cr/Au are evaporated for the substrate and top contact, respectively. Using a metal contact of 70 μm in diameter for bonding, most of the mesa surface is uncovered, leaving enough space for optical access.

TABLE II. Layer sequence of graded superlattices with variable well and barrier thicknesses. d denotes the nominal layer thickness.

Well	d (nm)	Material
	1.4	$Al_{0.35}Ga_{0.65}As$
1	7.0	GaAs
	0.9	$Al_{0.35}Ga_{0.65}As$
2	5.0	GaAs
	2.5	$Al_{0.35}Ga_{0.65}As$
3	3.6	GaAs
	3.3	$Al_{0.35}Ga_{0.65}As$
4	2.8	GaAs
	3.9	$Al_{0.35}Ga_{0.65}As$
5	2.2	GaAs
	4.5	$Al_{0.35}Ga_{0.65}As$
6	1.7	GaAs
	5.3	$Al_{0.35}Ga_{0.65}As$
7	1.2	GaAs
	6.1	$Al_{0.35}Ga_{0.65}As$
8	0.8	GaAs
	6.5	$Al_{0.35}Ga_{0.65}As$

We have performed photocurrent, electroreflectance, and photoluminescence spectroscopy on these samples. The experiments are performed in a cryostat keeping the temperature either at 5 K (PC and PL) or about 80 K (ER). The PC spectra are measured in a standard setup using a lock-in technique. The ER spectra are obtained in a standard setup at normal incidence using a square-wave modulation of 50 mV at 183 Hz. The PL spectra are detected by a liquid-nitrogen-cooled charge-coupled device array using an 1-m monochromator.

III. EXPERIMENTAL RESULTS

The parameters for both samples were chosen in order to achieve an electron miniband width at finite electric fields of 50–60 meV. The p^+-i-n^+ diode has a built-in voltage V_{BI} so that the flat band condition between the contact layers is actually achieved at about 1.6 V, if the back contact is

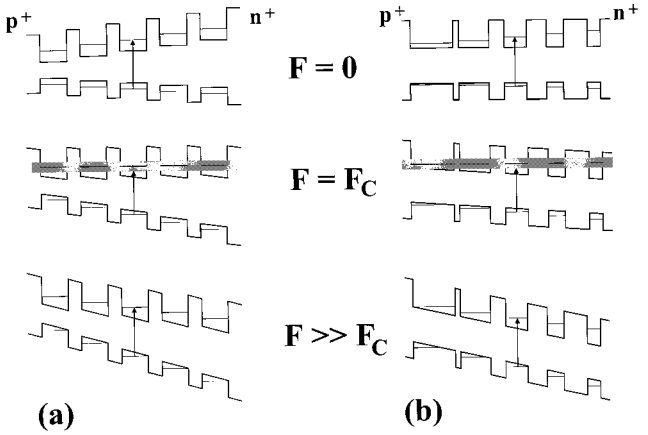

FIG. 1. Schematic conduction- and valence-band potential profile in a graded-gap superlattice with compositional grading (a) and variable well and barrier thicknesses (b) for different field strengths [top: zero field ($F=0$), center: miniband formation ($F=F_C$), bottom: large electric field, for which complete localization of conduction-band states occurs ($F \gg F_C$)].

grounded. The miniband is formed when the applied voltage is reduced to about 1.3 to 1.0 V. A schematic diagram of the conduction- and valence-band potential profile is shown in Fig. 1(a) for the compositionally graded and in Fig. 1(b) for the thickness graded superlattice. The top profile corresponds to the flat band condition, i.e., zero electric field ($F=0$). The center profile shows the formation of the miniband in the conduction band at finite electric fields ($F=F_C$). The bottom profile corresponds to very high electric fields, when the electron miniband is again destroyed ($F \gg F_C$). Note that the valence-band states never form a miniband for this polarity. If a voltage beyond the built-in voltage is applied, the valence-band states will form a miniband, while the conduction-band states will always be localized. However, since for this voltage regime electrons and holes are injected from the contacts into the intrinsic regime, the electric field will not be homogeneously distributed, making it difficult to observe the formation of a miniband. In order to study the miniband formation in the valence band, the contacts have to be interchanged.

In conventional SL's the destruction of the miniband can be observed by the blueshift of the energy gap with increasing electric field, since the individual quantum well states are located at the center of the miniband. The dispersion of an electron miniband in the tight-binding approximation can be written as

$$E(k_x,k_y,k_z)=\frac{\hbar^2(k_x^2+k_y^2)}{2m^*}+E_C-\frac{\Delta}{2}\cos(k_z d), \qquad (1)$$

where m^* denotes the in-plane effective mass, E_C the energy of the center of the miniband, Δ the width of the miniband, and d the superlattice period. When the miniband collapses, the energy of the lowest-energy state at $(k_x,k_y,k_z)=0$ is increased from $E_C-\Delta/2$ to E_C. Assuming that the heavy-hole state is always localized and neglecting excitonic effects, the energy gap of the superlattice therefore exhibits a blueshift of $\Delta/2$. Since in a graded-gap SL the miniband is formed at finite electric fields, the localization of the miniband states should be observable at higher as well as lower electric fields. Starting from zero electric field, the absorption spectrum should therefore display first a redshift of approximately $\Delta/2$ for each well of the graded-gap SL at the applied electric field, for which the miniband is formed. At higher electric fields the absorption edge should then exhibit the typical blueshift of the Wannier-Stark localization. Note that in contrast to conventional SL's the absorption spectrum should contain as many transitions as there are wells, since all of them occur at a different energy.

A. Photocurrent spectra

Absorption spectroscopy is rather difficult to perform on this type of sample, since the substrate has a smaller energy gap than the SL. In order to circumvent the problem of etching the substrate away, photocurrent spectroscopy is typically applied, since the contacts are also needed to apply the electric field. Photocurrent spectra of the compositionally graded SL are shown for selected voltages in Fig. 2(a). A clear modulation of the continuously increasing photocurrent by transitions from the individual wells of the graded-gap SL is observed. These transitions occur between the highest heavy-hole subband and the lowest electron subband or miniband (H11). However, at 0.7 V this modulation almost disappears and reappears for lower voltages, i.e., larger electric fields, again. This region probably corresponds to the transition from extended miniband to Wannier-Stark states. Taking the derivative of the PC, at least 13 transitions can be clearly identified.[14] The first transition region, i.e., from localized to extended states, cannot be observed with photocurrent spectroscopy, since the current in this field range is very small. The reason for this small photocurrent is that most electrons will not be able to reach the n^+ contact until the miniband is formed. Instead they will accumulate in the first well (or the enlarged well between the SL and the contact) and recombine with holes, which flow for all displayed voltages to the p^+ contact. Note that the spectra clearly show the two-dimensional density of states as expected for quantum wells. However, no excitonic effects are present. Furthermore, transitions of electrons with light-hole states are not resolved.

The photocurrent spectra of the thickness graded SL are very different. Several spectra for selected voltages are shown in Fig. 2(b). The spectra are clearly dominated by excitonic transitions. In addition to the heavy-hole peaks, weaker peaks are also present. Some of these peaks can be attributed to transitions between the highest light-hole subband and the lowest electron states (L11). At least six of the eight GaAs wells can be observed in the PC spectra. However, for the narrower wells the heavy- and light-hole transitions of adjacent wells begin to overlap. The transition from extended miniband to localized states is again expected at voltages between 1.0 and 0.7 V. In this range a strong reduction of the excitonic signal of the individual wells with respect to the background signal is clearly visible. This quenching of the excitonic signal could be a result of the ionization of the excitons by the electric field.

Looking at the field dependence of the peaks of the differentiated PC spectra as shown in Fig. 3 as a function of the applied voltage, no distinct redshift or blueshift of the tran-

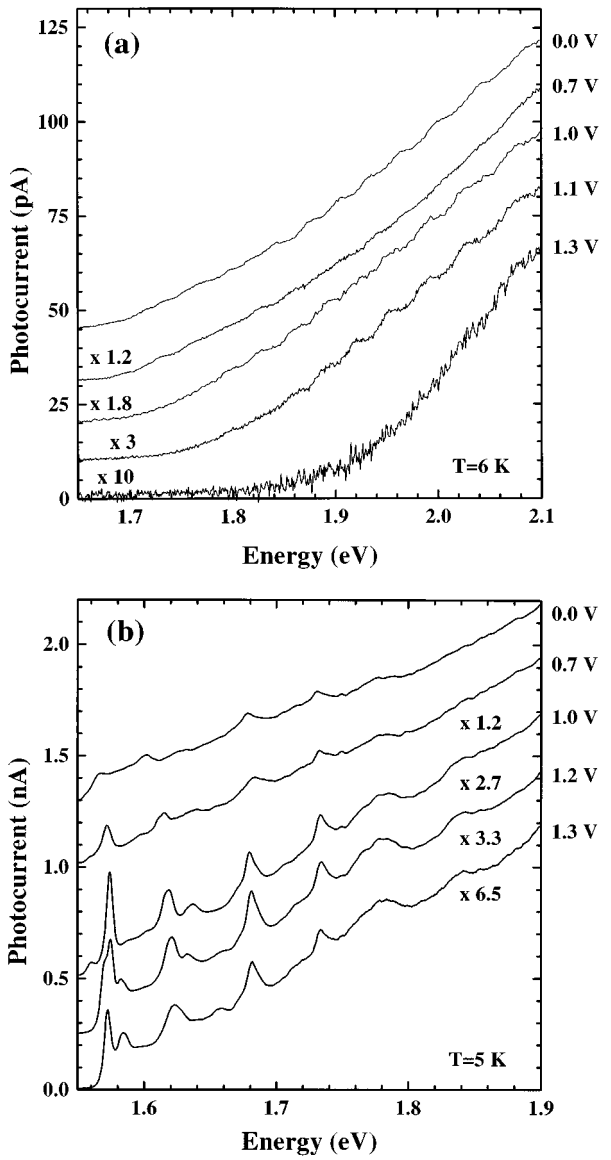

FIG. 2. Photocurrent spectra of the graded-gap superlattice with compositional grading (a) and with variable well and barrier thicknesses (b) for several applied voltages at 5–6 K. The different curves have been rescaled with the indicated factor.

sitions can be observed. A clear anticrossing or splitting occurs at about 1.2 V for the transiton of the largest well (1.573 eV). At the same time, the light-hole transition on the high-energy side (1.583 eV) disappears. This figure clearly shows the dominance of the excitonic effects up to quite large electric fields. At 0 V [cf. Fig. 2(b)] the excitonic effects are strongly reduced.

B. Electroreflectance spectra

In order to clearly demonstrate the formation of a miniband at finite electric fields, the graded-gap superlattice has to be investigated at all field strengths, even close to zero electric field, i.e., when the built-in voltage is compensated. This can be achieved by performing absorption measurements, which have some difficulty as discussed above. In order to remove the background signal, a differential technique such as differential PC or ER spectroscopy should be

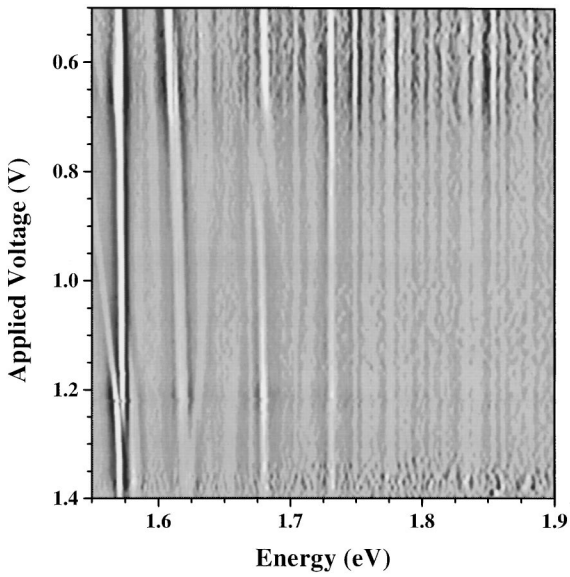

FIG. 3. Voltage dependence of the differentiated photocurrent spectra for the graded-gap superlattice with variable well and barrier thicknesses at 5 K. Dark areas correspond to large values of the derivative of the photocurrent. The voltage step is 10 mV.

applied. Differential PC spectroscopy has been performed on the compositionally graded SL. However, only the transition from extended miniband to Wannier-Stark states could be observed,[15,16] since no photocurrent is detected before the miniband is formed. ER has the advantage over any photocurrent or absorption related technique that it provides a signal at all field strengths without etching the substrate away. At the same time, it is differential. Although the ER signal is more complicated since it is composed of both absorption and refractive index changes inside the sample, the essential structures can easily be identified.

The electroreflectance spectra of the compositionally graded-gap SL have already been shown in Ref. 12. However, for a direct comparison it is necessary to put the field dependence side by side with the thickness graded SL. In Fig. 4(a) the voltage dependence of the ER spectra for the compositionally graded SL measured at 80 K are shown. The darker areas correspond to maxima of the normalized ER signal. We are mainly interested in the field dependence of the observed transitions and not so much in the detailed shape of the spectra. At 1.6 V, close to the flatband voltage, all 15 wells contribute to the ER signal in strong contrast to the PC spectra [cf. Fig. 2(a)]. Increasing the electric field, no change is observed up to about 1.45 V. Between 1.45 and 1.35 V the ER maxima exhibit a clear redshift by 17 meV. The vertical dashed line is included to clearly visualize the redshift for one particular well. This region corresponds to the formation of the miniband, which exists to about 1.15 V. Between 1.15 and 1.05 V the spectra show a rather complex line shape due to the interaction of the Wannier-Stark ladder transitions. For even larger fields the individual lines are blueshifted by 17 meV. These spectra clearly demonstrate the formation of a miniband at finite electric fields. It is most clearly observed in the energy range above 1.78 eV. For smaller energies, the quantum well energy levels cannot be accurately aligned, and the corresponding wave functions remain partially localized. Numerical simulations of the differ-

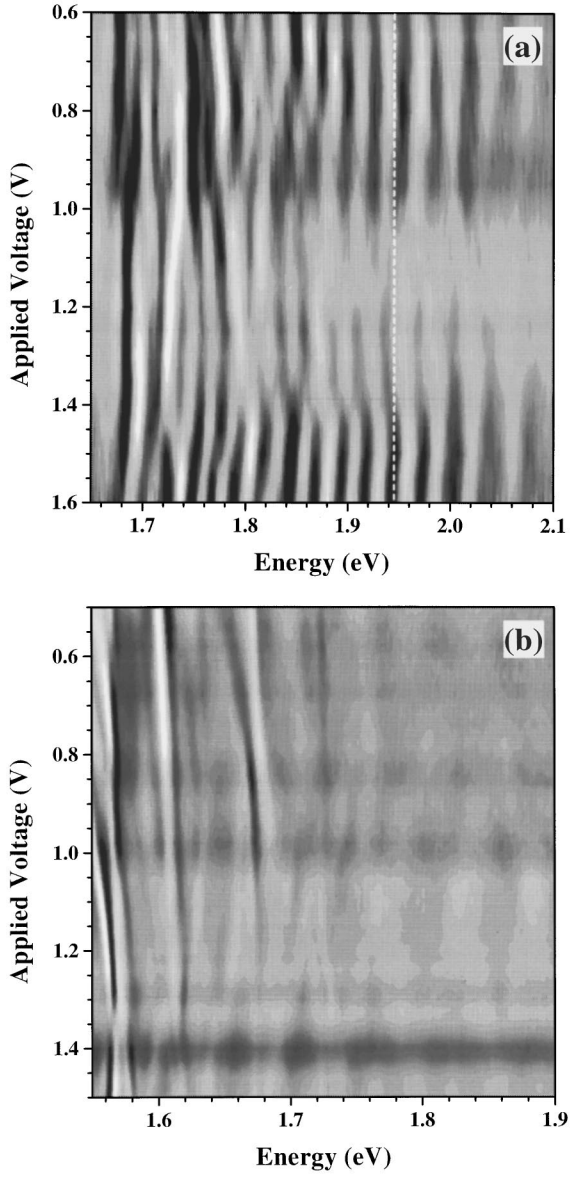

FIG. 4. Voltage dependence of the electroreflectance spectra for the graded-gap superlattice with compositional grading (a) and with variable well and barrier thicknesses (b) at 80 K. Dark areas correspond to maxima of the electroreflectance signal. The vertical dashed line in (a) is used to indicate the energy shift, when the miniband is formed. The voltage step is 50 mV in (a) and 20 mV in (b).

ential absorption spectra, which confirm this interpretation, will be discussed below. Since in a graded-gap SL each well produces in the miniband and fully localized regime a transition at a different energy, the Wannier-Stark transition regime, which in a conventional SL is characterized by a large number of observable transitions, becomes rather structureless in the graded-gap SL, since the oscillator strength is distributed over many more transitions.

In Fig. 4(b) the voltage dependence of the normalized ER spectra for the thickness graded SL measured at 80 K is shown. As expected from the PC spectra, the ER spectra are also dominated by excitonic effects. At least four wells can be directly observed in the ER spectra. The strongest ER signal originates from the largest well at about 1.58 eV. It

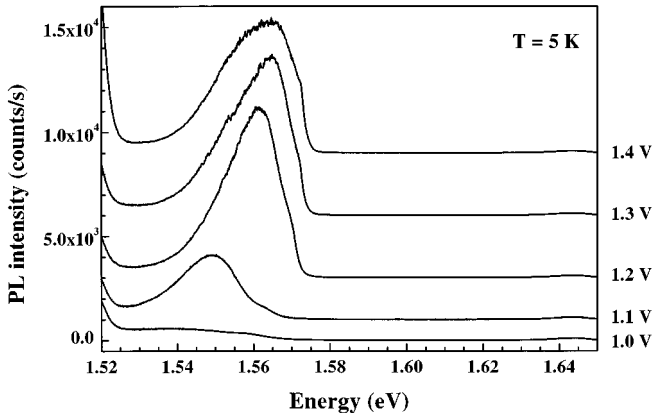

FIG. 5. Photoluminescence spectra of the graded-gap superlattice with variable well and barrier thicknesses at 5 K for several applied voltages at an excitation energy of 1.78 eV. No signal was detected at energies above 1.65 eV. The spectra have been vertically shifted so that for each spectrum the signal at high energies corresponds to the zero line signal.

contains two transitions, which are not completely resolved. In addition to the H11 and L11 transitions, also higher allowed and forbidden transitions can contribute to the spectra. The small energy shift with respect to the differentiated PC spectra (Fig. 3) is due to the different temperature. At higher energies, the broadening of the different transitions and the degree of overlap increases. At the same time, the amplitude of the ER signal decreases. Therefore, it is more difficult to resolve transitions originating from the narrower wells. The miniband is probably formed at about 1.35 V and destroyed at about 1 V, since a strong change in the spectrum for the largest well transition is observed for these voltages. However, due to the strong excitonic transitions, the formation of the miniband is not so clearly seen as for the compositionally graded sample. Below we will compare the observed spectra with the spectral dependence of the calculated differential absorption coefficient.

C. Photoluminescence spectra

The compositionally graded SL does not show any PL signal for applied voltages below the built-in voltage or any electroluminescence signal for applied voltages above V_{BI}. We attribute the absence of any PL signal to the Al content in the wells and barriers. This might lead to a poor interface quality resulting in enhanced nonradiative recombination. However, even the first well, which is pure GaAs, does not show any luminescence. In the thickness graded SL the interface quality should be greatly improved and a PL signal is expected to appear. The PL spectra for selected applied voltages of the thickness graded SL are shown in Fig. 5. The spectra were taken at 5 K. In the energy range of the graded-gap SL only a single PL line at 1.56 eV is observed. Its intensity is strongly quenched between 1.2 and 1.0 V. This behavior can be understood as follows. Before the miniband is formed, all photoexcited electrons will move to the widest (first) well due to the graded energy gap of the structure. At the same time photoexcited holes will always move to the widest well for voltages below V_{BI}. Due to the photon energy used, only the first four wells are excited. Photoexcited

electrons will therefore only recombine in the widest well, since the transport time from any well in the superlattice to the first well is much shorter than the recombination lifetime. When the miniband is formed, photoexcited electrons can now move to the back contact and the PL signal of the first well is strongly quenched. At higher fields, when the miniband is destroyed again, the electrons still move very quickly to the back contact and recombination of electrons and holes is suppressed. This effect was also observed by Cao *et al.*[13] in a similarly designed graded-gap SL. However, they used a very large intrinsic region so that the applied voltages were much higher. This observation clearly shows that PL and PL excitation spectroscopy are not very useful techniques to investigate graded-gap SL's. The strength of the PC and PL signals is strongly influenced by the transport properties. However, the ER spectra are not affected by transport and only reflect the intrinsic band structure properties of the investigated system.

IV. CALCULATED ABSORPTION SPECTRA

In order to confirm the interpretation of the experimental results calculations of the absorption spectra for both the compositionally graded and the well width graded structure have been performed. In both cases the superlattice structures have been terminated by barrier layers of 10-nm width on either side and then embedded between infinite barriers. A comparison with the results for the full structure including top and bottom spacer and doping layers showed that a huge number of additional transitions would occur in the spectra, but the structures resulting from the superlattice region remain basically unaffected. In a first step the complete set of electron, heavy-hole, and light-hole eigenstates in the relevant energy range have been calculated using a transfer matrix technique (see, e.g., Ref. 17). An effective mass method has been used for both the electron and hole states neglecting valence-band coupling. The relevant wave functions are almost completely confined in the superlattice region, confirming the assumption that the explicit boundary conditions of the problem are only of minor importance. In a second step the optical absorption coefficient has been calculated, summing up the transition probabilities of all possible combinations of electron and hole states multiplied by the appropriate momentum matrix elements and the two-dimensional combined density of states.[18] The electron-hole Coulomb interaction has been neglected. A Gaussian broadening function has been added with an empirical broadening parameter chosen to fit the line widths observed in the experiment.

Figure 6(a) shows the differentiated absorption spectra $\partial\alpha(\omega)/\partial\omega$ of the compositionally graded superlattice as a function of energy and electric field. Although the results cannot be directly compared with the ER spectra of Fig. 4(a), there is a good agreement with respect to the essential structures. The transition from the Wannier-Stark to the miniband regime is excellently reproduced both on the low-field ($F \approx 10$ kV/cm) and the high-field side ($F \approx 65$ kV/cm), the signature being a redshift and a smoothing of the structures in the intermediate field range. Similar to the experimental observations the low-energy transitions do not show this behavior, but remain relatively strong for all fields. This indicates that the wave functions of the wide wells remain

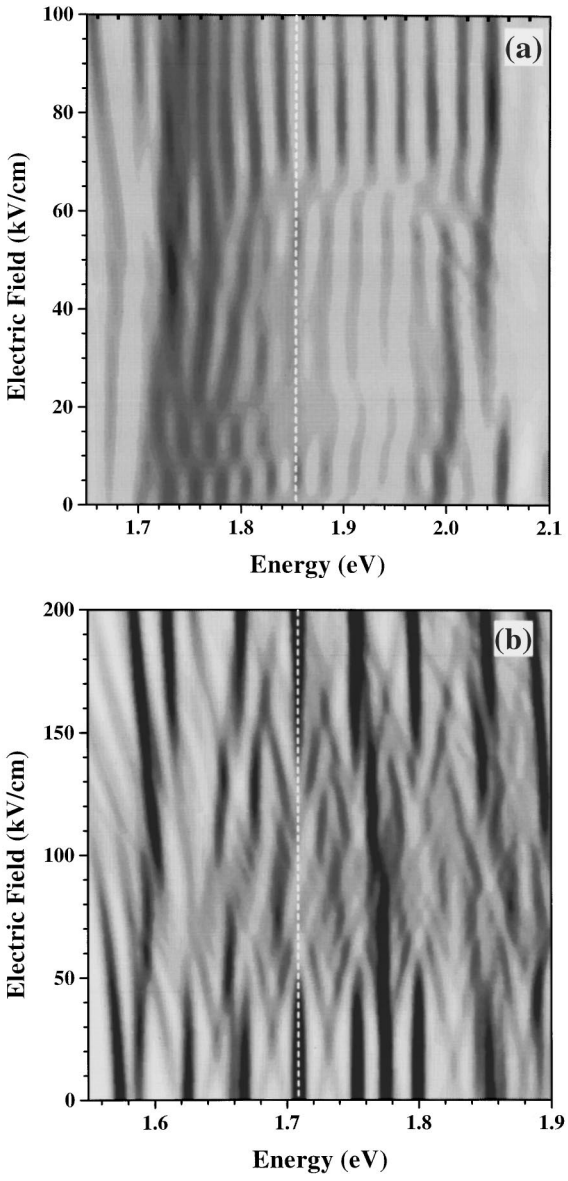

FIG. 6. Calculated voltage dependence of the differential absorption coefficient for the graded-gap superlattice with compositional grading (a) and with variable well and barrier thicknesses (b). Dark areas correspond to maxima of the differential absorption coefficient. Excitonic effects have not been taken into account. The vertical dashed line is used to indicate the energy shift, when the miniband is formed. The electric field step is 2.5 kV/cm.

mostly localized for all fields as a consequence of poor alignment of the energy levels with the smaller wells. In contrast to the compositionally graded superlattice the agreement of the numerical results with the experimental results for the well width graded structure is only poor [Fig. 6(b)]. The calculations exhibit a number of transitions that are split and intermixed, forming a complicated pattern in the intermediate field range ($F \approx 50-140$ kV/cm), whereas the experimental spectra basically show the spatially direct transitions [Fig. 4(b)]. The basic reason for this discrepancy may be the fact that the interwell coupling is less pronounced in this structure, yielding a strongly disturbed miniband, while the excitonic effects are clearly enhanced. Thus, the Coulomb localization effect seems to exceed the wave-function delo-

calization induced by level coupling. As a result, the Coulomb interaction stabilizes the intrawell excitons and suppresses the interwell transitions. As the Coulomb interaction is neglected in the calculations, this effect does not occur in the theoretical spectra.

V. SUMMARY

The formation of an electron miniband at finite electric fields has been investigated in two different types of graded-gap superlattices in the material system $GaAs/Al_xGa_{1-x}As$. In one sample the graded-gap SL is achieved by a compositional grading. In this system, where no excitonic effects are observed, the formation of the miniband can be directly observed by electroreflectance spectroscopy. The Wannier-Stark transition regions at small and large fields are confined to a much smaller field range than in conventional superlattices. In the other sample, the graded-gap SL is achieved by changing the well and barrier thicknesses. In contrast to the compositionally graded system, the photocurrent and electroreflectance spectra of this system are dominated by excitonic effects. The miniband formation in the intermediate-field range is confirmed by calculated absorption spectra for the compositionally graded superlattice. For the well width graded structure the poor observability of miniband formation is attributed to strong exciton localization effects.

ACKNOWLEDGMENTS

We would like to thank A. Fischer for sample growth. One of us (H.T.G) would like to thank the Research Center for Quantum Effect Electronics at the Tokyo Institute of Technology for its hospitality during the preparation of the manuscript. This work was supported in part by BMBF of the Federal Republic of Germany.

[1] L. Esaki and R. Tsu, IBM J. Res. Dev. **14**, 61 (1970).
[2] E. E. Mendez, F. Agulló-Rueda, and J. M. Hong, Phys. Rev. Lett. **60**, 2426 (1988).
[3] F. Capasso, K. Mohammed, and A. Y. Cho, Appl. Phys. Lett. **48**, 478 (1986).
[4] H. T. Grahn, H. Schneider, W. W. Rühle, K. v. Klitzing, and K. Ploog, Phys. Rev. Lett. **64**, 2426 (1990).
[5] See, e.g., *Semiconductor Superlattices, Growth and Electronic Properties*, edited by H.T. Grahn (World Scientific, Singapore, 1995).
[6] F. Capasso, H. M. Cox, A. L. Hutchinson, N. A. Olsson, and S. G. Hummel, Appl. Phys. Lett. **45**, 1193 (1984).
[7] D. H. Lee, S. S. Li, N. J. Sauer, and T. Y. Chang, Appl. Phys. Lett. **54**, 1863 (1989).
[8] K. Kurihara, T. Numai, I. Ogura, A. Yasuda, M. Sugimoto, and K. Kasahara, J. Appl. Phys. **73**, 21 (1993).
[9] Y. Shiraishi, N. Furuhata, and A. Okamoto, J. Appl. Phys. **76**, 5099 (1994).
[10] J. Faist, F. Capasso, C. Sirtori, D. L. Sivco, A. L. Hutchinson, and A. Y. Cho, Appl. Phys. Lett. **66**, 538 (1995).
[11] S. E. Ralph, F. Capasso, and R. J. Malik, Phys. Rev. Lett. **63**, 2272 (1989).
[12] U. Behn, N. Linder, H. T. Grahn, and K. Ploog, Phys. Rev. B **51**, 17 271 (1995).
[13] S. M. Cao, M. Willander, A. A. Toropov, T. V. Shubina, B. Ya. Mel'tser, S. V. Shaposhnikov, P. S. Kop'ev, P. O. Holtz, J. P. Bergman, and B. Monemar, Phys. Rev. B **51**, 17 267 (1995).
[14] F. Agulló-Rueda, H. T. Grahn, A. Fischer, and K. Ploog, Phys. Rev. B **45**, 8818 (1992).
[15] F. Agulló-Rueda, A. D'Intino, K. H. Schmidt, G. H. Döhler, H. T. Grahn, and K. Ploog, Europhys. Lett. **23**, 283 (1993).
[16] H. T. Grahn, F. Agulló-Rueda, A. D'Intino, K. H. Schmidt, G. H. Döhler, and K. Ploog, Solid State Electron. **37**, 835 (1994).
[17] C. Weisbuch and B. Vinter, *Quantum Semiconductor Structures: Fundamentals and Applications* (Academic Press, San Diego, 1991).
[18] G. Bastard, *Wave Mechanics Applied to Semiconductor Heterostructures* (Les Éditions de Physique, Les Ulis, France, 1989).